

# Giant shift upon strain on the fluorescence spectrum of $V_N N_B$ color centers in $h$ -BN

Song Li, Jyh-Pin Chou, and Alice Hu

*Department of Mechanical Engineering, City University of Hong Kong, Hong Kong SAR, China*

Martin B. Plenio

*Institute of Theoretical Physics and IQST, Albert-Einstein-Allee 11, Ulm University, 89069 Ulm, Germany*

Péter Udvarhelyi

*Wigner Research Centre for Physics, P.O. Box 49, H-1525 Budapest, Hungary and  
Eötvös Science University, Pázmány Péter Sétány 1/A, H-1117 Budapest, Hungary*

Gergő Thiering

*Wigner Research Centre for Physics, P.O. Box 49, H-1525 Budapest, Hungary*

Mehdi Abdi

*Department of Physics, Isfahan University of Technology, Isfahan 84156-83111, Iran*

Adam Gali

*Wigner Research Centre for Physics, P.O. Box 49, H-1525 Budapest, Hungary and  
Budapest University of Technology and Economics, Budafoki út 8, H-1111 Budapest, Hungary  
(Dated: December 21, 2024)*

We study the effect of strain on the physical properties of the nitrogen antisite-vacancy pair in hexagonal boron nitride ( $h$ -BN), a color center that may be employed as a quantum bit in a two-dimensional material. With group theory and ab-initio analysis we show that strong electron-phonon coupling plays a key role in the optical activation of this color center. We find a giant shift on the zero-phonon-line (ZPL) emission of the nitrogen antisite-vacancy pair defect upon applying strain that is typical of  $h$ -BN samples. Our results provide a plausible explanation for the experimental observation of quantum emitters with similar optical properties but widely scattered ZPL wavelengths and the experimentally observed dependence of the ZPL on the strain.

## I. INTRODUCTION

Quantum emissions from two-dimensional materials has recently received considerable and rapidly rising interest of researchers in both condensed matter and quantum optics [1–3] as these systems provide a potential basis for emerging technologies such as quantum nanophotonics [4–6], quantum sensing [7–9], and quantum information processing [10, 11]. The observation of single-photon emitters (SPEs) in hexagonal boron nitride ( $h$ -BN) has added a fascinating new facet to the research field of layered materials [12]. The wide band gap of  $h$ -BN makes it an insulator that can host high quality emitters and allows for combination with other materials as substrates [13]. The experiments for exploring the nature of the emission of these color centers started with their first observations [10, 14–25] and recent theoretical works have provided evidence that the SPEs are indeed color centers, i.e. local point defects [26–30].

Despite the considerable efforts that have been directed at the experimental exploration of these SPEs so far, a thorough theoretical understanding of the properties of the emitters that have been experimentally observed remains to be developed. Especially, the fact that many emitters appear at the edges of  $h$ -BN flakes and wrinkles on them [31, 32] motivates the investigation on the effect of strain on these emitters. Furthermore, the quantum

emitters have shown magnetic properties in some experiments [33–36], while in other experiments non-magnetic behaviour was found [21].

The most commonly observed quantum emitters exhibit emission in the visible, where competing theoretical models [27, 37] exists in the literature. It has been suggested recently, based on the similarities of the optical lifetimes of the observed quantum emitters [38], that two types of quantum emitters in the visible region may occur in  $h$ -BN, and the widely scattered zero-phonon-line (ZPL) energies might be attributed to external perturbations. One of the key candidates for this external perturbation is the local strain that may vary significantly in the  $h$ -BN samples, in particular, in polycrystalline  $h$ -BN samples. In another recent work, on the other hand, four different types of emitters have been found by means of combined cathodoluminescence and photoluminescence study where the applied stress did not change the brightness of emitters and the shift in ZPL was in the 10 meV region [39]. Yet another experiment also found a relatively small shift upon applied stress on a given emitter [40].

These seemingly contradictory observations and the lack of a conclusive theoretical prediction motivates the study of the effect of strain on point defects in  $h$ -BN based on the assumption that point defects are the origin of the observed quantum emitters. Furthermore, a

thorough understanding of the electron-strain coupling properties also forms a rigorous theoretical basis for proposed spin- and electro-mechanical systems for control and manipulation of a mechanical resonator by means of spin-motion coupling [11, 41, 42]. Group-theory analysis in combination with ab-initio Kohn-Sham density functional theory (DFT) simulations can be a very powerful tools for understanding the coupling between the optical emission and strain. So far the electron-strain coupling in *h*-BN emitters has been studied with limited accuracy [40] by monitoring only the change in Kohn-Sham levels and the states that do not directly provide the ZPL energy in the PL spectrum monitored in the experiments.

Here we study the effect of strain on the ZPL emission of a key color center in *h*-BN, the nitrogen antisite-vacancy pair defect, by means of group theory and advanced DFT calculations, which can act as a quantum emitter with exhibiting a ZPL emission at around 1.9 eV (645 nm) [27]. We report a giant, 12 eV/strain ZPL-strain coupling parameter for this quantum emitter which results in about 100 nm scattering of the ZPL emission with  $\pm 1\%$  strain in *h*-BN sample. The physical origin of this giant effect is the strong electron-phonon coupling in *h*-BN. This result implies that local perturbations for vacancy type defects can seriously affect their optical spectrum and provide an explanation for the zoo of reported quantum emitters in the visible region.

## II. RESULTS

The sensitivity of the optical ZPL emission to the applied local strain greatly depends on the microscopic configuration of the point defect in *h*-BN. Here, we put our focus on the neutral nitrogen antisite-vacancy pair defect,  $V_N N_B$ , which was first suggested as a candidate of the observed single-photon emissions [10] and then thoroughly studied as one of the feasible quantum emitter in the visible with  $S = 1/2$  spin state [27]. The optical properties of this defect have been examined from various theoretical methods and point of view [27, 43–45]. The defect has a  $C_{2v}$  symmetry before relaxation of the atoms, and introduces three levels in the energy band gap that are labeled as  $a_1$ ,  $b_2$  and  $b'_2$  owing to their irreducible symmetry representation. These energy levels are occupied by three electrons [see Figs. 1 and 2]. The two lowest-energy spin-preserving optical transitions are the following: in the spin majority channel the electron from  $b_2$  may be promoted to  $b'_2$  or in the spin minority channel the electron from  $a_1$  may be promoted to  $b_2$ . It is found that the  $a_1 \leftrightarrow b_2$  has lower energy than  $b_2 \leftrightarrow b'_2$  [27, 43, 44]. However, for the defect with the  $C_{2v}$  symmetry the  $a_1 \leftrightarrow b_2$  optical transition has a very small optical transition in-plane dipole moment [44]. Indeed, we also find this behavior in our own DFT calculation (see Supplementary Figure S1). We indeed notice that  $b_2$  and  $b'_2$  states have wavefunctions that extend out-of-plane [see Fig. 1(b)], and therefore, can couple to phonon

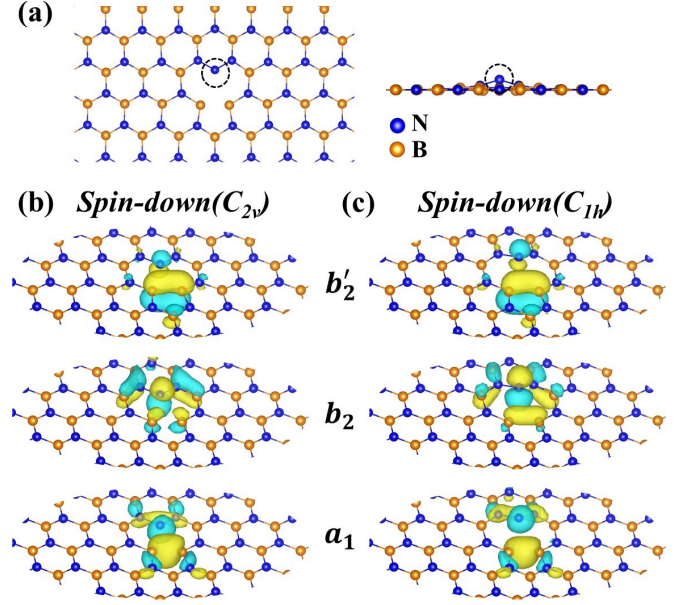


FIG. 1. (a) The geometry of  $V_N N_B$  defect in the ground state. Top view (left) and side view (right). The dashed circle denotes the impurity nitrogen atom. The defect is out-of-plane and exhibits  $C_{1h}$  symmetry. (b) The  $a_1$ ,  $b_2$  and  $b'_2$  defect states in  $C_{2v}$  geometry. (c) The defect states in the  $C_{1h}$  symmetry with the same energy order as those in (b). As can be seen the  $a_1$  and  $b_2$  wavefunctions in  $C_{2v}$  symmetry are mixed in  $C_{1h}$  symmetry.

modes that drive the atoms out-of-plane, the membrane modes. There is an unpaired electron in both  $B_2$  ground state and  $B'_2$  excited state placed on the  $b_2$  and  $b'_2$  orbital, respectively, that induce an out-of-plane geometry distortion. Therefore, the defect does not preserve the planar structure and the nitrogen antisite moves out from the plane when the complex assumes its  $B_2$  or  $B'_2$  states reducing the symmetry of the defect to  $C_{1h}$  [see Fig. 1(a)]. This geometry is about 100 meV lower in energy than the  $C_{2v}$  configuration which reveals the strong coupling of the defect electrons to the membrane mode phonons. This result basically agrees with previous DFT calculations [46]. On the other hand, the  $a_1$  orbital has a wavefunction that extends in the plane of the lattice. Therefore, when the hole is left at this orbital in the  $A_1$  excited state, then the coupling to the membrane phonons is switched-off and the defects  $C_{2v}$  symmetry is retrieved. For the sake of simplicity, here we use the  $C_{2v}$  symmetry labels for both configurations.

Owing to the rearrangement of the ions, the  $B_2(C_{1h}) \leftrightarrow A_1(C_{2v})$  optical transition assumes a dipole moment symmetry similar to that of  $B_2(C_{1h}) \leftrightarrow B'_2(C_{1h})$  transition. This becomes clear from Fig. 1(c) where the wavefunctions  $b_2$  and  $a_1$  are shown for the  $C_{1h}$  configuration. In fact, both of them transform as  $A'$  in the  $C_{1h}$  configuration, and therefore, are coupled via the in-plane (the stronger component) polarization. As a consequence, the lowest energy fluorescence is expected

to occur as a radiative decay from the  $A_1(C_{2v})$  excited state to the  $B_2(C_{1h})$  ground state because  $A_1$  excited state has lower energy than that of  $B'_2$  excited state [27]. *This result constitutes the optical activation of a color center in  $h$ -BN by means of a strong electron-phonon coupling.* Consequently, it becomes important to study the strain dependence of the ZPL emission for the  $B_2(C_{1h}) \leftrightarrow A_1(C_{2v})$  optical transition. Details on the strain dependence for the higher energy transition is shown in the Supplementary Note 2.

It is intriguing to carry out group theory analysis before starting the numerical ab-initio calculations. The detailed general description about the multi-electron configurations and their interaction with strain can be found in the Methods, that we apply to the  $V_N N_B$  quantum emitter. The analysis is performed for the  $C_{2v}$  symmetry as the excited state transforms within  $C_{2v}$  symmetry whereas the  $C_{1h}$  ground state follows the same analysis taking into account the fact that  $C_{1h}$  is a subgroup of the  $C_{2v}$  symmetry. Within  $C_{2v}$  symmetry for the axial strain, the ZPL shift upon strain is given by

$$\delta = \hat{\varepsilon}^{A_1} [\langle b_2 | \hat{\Delta}^{A_1} | b_2 \rangle - \langle a_1 | \hat{\Delta}^{A_1} | a_1 \rangle], \quad (1)$$

where  $\hat{\varepsilon}^{A_1}$  is the strain tensor applying the strain parallel to the  $C_2$  symmetry axis (axial strain) and  $\hat{\Delta}^{A_1}$  is associated with the energy shifts for the corresponding electronic states (see Methods). The  $C_{1h}$  configuration can then be described as an out-of-plane distortion due to a built-in strain which acts perpendicular to the basal plane. This mixes  $a_1$  and  $b_2$  orbitals through  $B_2$  component of the strain as explained in Methods. Since the energy spacing between the  $a_1$  and  $b_2$  levels is much larger than the typical deformation values this mixture should not significantly alter the energy shift of  $\delta$  upon applying basal uniaxial strain. Hence, the energy shift in Eq. (1) is a good approximation. This ZPL energy shift is expected to depend linearly on strain for the  $B_2(C_{1h}) \leftrightarrow A_1(C_{2v})$  optical transition. The magnitude of the strain-ZPL coupling as a function of the orientation of the applied uniaxial strain cannot be determined by means of group theory. We, therefore, apply DFT simulations to quantify the strength of the strain-ZPL coupling for  $V_N N_B$  emission.

We calculate the ZPL energy as the total energy difference between the excited state and the ground state in the global energy minimum of the corresponding electronic configuration (see Method). The strain is modelled by changing the lattice constant of the employed supercell [see Fig. 2(a), where the parallel (red) and perpendicular (black) components of the strain are depicted]. The corresponding curves for the ZPL shift are plotted in Fig. 2(b) as a function of the applied strain. As expected, the curves are quasi-linear within  $[-1; +2]\%$  strain region, where we use  $-$  and  $+$  for compressive and tensile strain, respectively. For both strain directions, we obtain a giant, 12 eV/strain shift in the ZPL energy which results in a huge variation in the emission wavelength as a function of strain. For this quantum emitter, the ten-

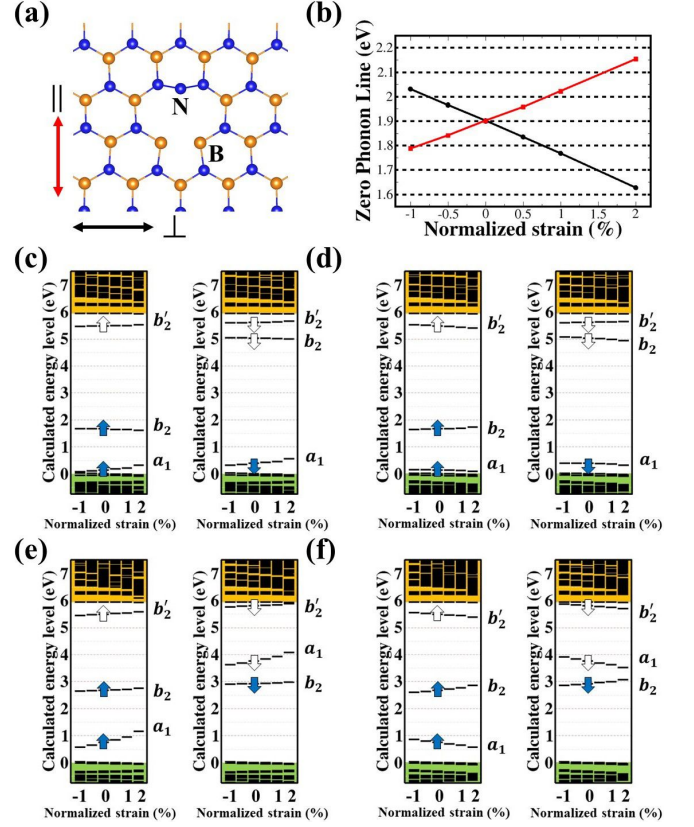


FIG. 2. (a) The simplified cartoon of  $V_N N_B$  defect in  $h$ -BN. The defect is not planar and exhibits  $C_{1h}$  symmetry in the ground state. The black and red arrow denote the directions of uniaxial strain perpendicular ( $\perp$ ) and parallel ( $\parallel$ ) to the  $C_2$  main axis, respectively. (b) The ZPL evolution as a function of external strain for  $a_1$  to  $b_2$  transition. The black and red line denote the directions of strain perpendicular ( $\perp$ ) and parallel ( $\parallel$ ) directions. The energy level at ground state with  $C_{1h}$  symmetry evolution as a function of external strain for perpendicular (c) and parallel (d) directions, respectively. The energy level at excited state ( $a_1$  to  $b_2$ ) with  $C_{2v}$  symmetry evolution as a function of external strain for perpendicular (e) and parallel (f) directions, respectively.

tile axial (perpendicular) uniaxial strain causes blueshift (redshift) in the ZPL emission.

In order to further study these results, we plot the shift of the defect levels upon the applied strain in the corresponding ground and excited states in Fig. 2(c)-(f). Upon applying tensile axial strain, the  $a_1$  level in the ground state shifts down whereas the occupied  $b_2$  level shifts up in the ground and excited electronic configurations, respectively. This will result in a blueshift in the ZPL. Upon applying tensile perpendicular strain, the  $a_1$  level shifts up steeply whereas the occupied  $b_2$  level moderately shifts up in the ground and excited electronic configurations, respectively. As a consequence, the two levels approach each other upon applying this strain which results in a redshift in the ZPL energy. This is in agreement with the observations reported in Ref. [40] where



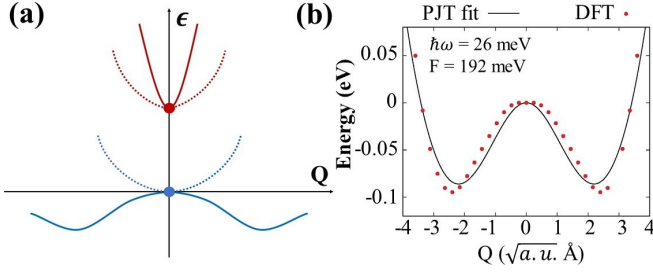


FIG. 3. (a) Pseudo Jahn-Teller (PJT) effect between the excited state (red) and ground state (blue). Dashed line: before electron-phonon coupling; straight line: after electron-phonon coupling.  $\epsilon$  is the total energy of the system whereas  $Q$  is the selected configuration coordinate. (b) The calculated adiabatic potential energy surface of the  $^2B_2$  ground state. The line is a fit of PJT model (see text), where the resultant values are  $F=192$  meV and  $\hbar\omega=26$  meV. The standard deviation is less than 2%.

the ZPL energy shift of the studied emitters exhibit a linear dependence on the applied strain. Furthermore, the three different possible orientations of the defect axis and our results on the blueshift (redshift) of the emission line for armchair (zigzag) strain explains the experimentally observed behavior [40].

### III. DISCUSSION

We find that the phonon modes with atoms moving out-of-plane, i.e., membrane modes, play a crucial role in the optical activation of the  $V_N N_B$  defect in  $h$ -BN. These membrane  $B_2$  phonons couple the  $^2A_1$  excited state and  $^2B_2$  ground state where the ground state will be unstable at the  $C_{2v}$  symmetry configuration and is distorted to  $C_{1h}$  configuration, whereas the excited state remains stable at  $C_{2v}$  configuration. This suggest a strong pseudo Jahn-Teller (PJT) [47] system which is illustrated in Fig. 3(a). We depict the adiabatic potential energy surface (APES) of the  $^2B_2$  ground state of  $V_N N_B$  in Fig. 3(b) as obtained by HSE DFT calculations. We note that DFT calculation with a less accurate semilocal functional than HSE (see Method) obtained a similar APES in a previous study [46]. The Jahn-Teller energy is 95 meV. The solution of this strongly coupled electron-phonon system [47] is

$$\epsilon_{\pm}(Q) = \frac{1}{2}M\omega^2Q^2 \pm (\Delta^2 + F^2Q^2)^{\frac{1}{2}}, \quad (2)$$

where  $Q$  is the normal coordinate of the effective phonon mode  $\omega$  with the corresponding mass  $M$ ,  $\Delta$  is the energy gap between the ground state and excited state at the high symmetry point ( $C_{2v}$  configurations) and  $F$  is the strength of electron-phonon coupling. In the dimensionless generalized coordinate system we obtain  $F=192$  meV and  $\hbar\omega=26$  meV. This electron-phonon coupling parameter is about  $2.5\times$  larger than that of NV center in dia-

mond [48]. This indicates a giant electron-phonon interaction for the vacancy type defects in  $h$ -BN. We solved the electron-phonon PJT system quantum mechanically and found that the jumping rate between the two minima is 8.4 kHz. This is a relatively slow rate where the optical Rabi-oscillation between the ground and excited states should be more than two orders of magnitude faster (see Supplementary Note 3). This means that the ground state of  $^2B_2$  is a static PJT system, and the ground state indeed exhibits low  $C_{1h}$  symmetry.

We note here that strong electron-phonon interaction with membrane phonons play an important role in the activation of intersystem crossing process in boron-vacancy optically detected magnetic resonance center [49]. This type of phonon modes can be found only in two-dimensional solid state systems. These findings demonstrate that the membrane phonon modes are major actors in the magneto-optical properties of solid state defect quantum bits and single photon emitters.

The strong electron-phonon interaction implies that the optical properties of vacancy type quantum emitters in  $h$ -BN can vary significantly with strain. Indeed, our DFT simulations show a giant shift in the ZPL emission at strain values that can appear in  $h$ -BN. This might be harnessed to use this quantum emitter for realizing stress detector at the nanoscale as well as nanomechanical devices for quantum technologies.

### IV. SUMMARY AND CONCLUSION

In this paper we performed a thorough group theory analysis and density functional theory calculations on the effect of strain on nitrogen antisite-vacancy color center in  $h$ -BN. We find a very strong electron-phonon interaction that can activate photoluminescence, and is responsible for the giant ZPL shift upon applied strain. The behavior of the strain-induced energy shift is correlated with the experimental observations further revealing their microscopic nature.

### V. METHODS

#### A. Group theory analysis on strain

In this section we provide a formulation that describes effect of local strain of the point defects. The derived Hamiltonian is general and is then applied to the  $V_N N_B$  quantum emitter in  $h$ -BN.

When considering point defects as candidates of the color centers in  $h$ -BN, the local strain manifests itself in modifying the atomic distances, which in turn, leads to the modification of the molecular orbitals (MOs) around the defect. Any change in the properties of MOs result in a redistribution of the energy states in the band structure of the host solid. Therefore, the strain directly couples

TABLE I. The configuration, symmetry, and spin multiplicity of the ground and two lowest excited states of neutral  $V_N B_N$ .

configuration	label	symmetry
$[a_1]^2[b_2]^1[b'_2]^0$	${}^2B_2$	$C_{1h}$
$[a_1]^1[b_2]^2[b'_2]^0$	${}^2A_1$	$C_{2v}$
$[a_1]^2[b_2]^0[b'_2]^1$	${}^2B'_2$	$C_{1h}$

to the electronic degrees-of-freedom of the color center. The coupling strength is called deformation potential.

We derive the Hamiltonian of the defect under local strain in the following way: We start by assuming that the color center is composed of  $N_e$  valance electrons that are mostly isolated from the rest of lattice and gather around  $N_n$  nuclei forming up the defect. Note that this is a fairly good assumption by looking at the MOs drawn by DFT belonging to the defect states [27]. The attractive Coulomb energy imposed from nuclei on the electrons is then given by

$$V_{Ne} = \sum_{j=1}^{N_e} \sum_{k=1}^{N_n} V_{jk}(\mathbf{X}_k, \mathbf{x}_j) \approx - \sum_j \sum_k \frac{Z'_k e^2}{R_{jk}}, \quad (3)$$

where  $R_{jk} = |\mathbf{X}_k - \mathbf{x}_j|$  with  $\mathbf{X}_k$  position of the nuclei, while  $\mathbf{x}_j$  denotes location of the  $j$ th electron. Here,  $Z'_k$  is the effective atomic number (screened nuclear charge) of the ion. The local strain displaces ions involved in the point defect  $\mathbf{X} \rightarrow \mathbf{X} + \delta\mathbf{X}$  and thus their Coulomb interaction. In the first order of accuracy we get  $V(|\mathbf{X} - \mathbf{x}|) \rightarrow V(|\mathbf{X} + \delta\mathbf{X} - \mathbf{x}|) \approx V(R) + [\nabla V(R)]_0 \cdot \delta\mathbf{X}$ , where  $\delta\mathbf{X}$  is the infinitesimal displacement of the nuclei imposed by the local strain. The value of displacement is obtained by  $\delta\mathbf{X} = \mathbf{X} \cdot \hat{\varepsilon}$  with the strain tensor  $\hat{\varepsilon}$ . The electron-strain interaction Hamiltonian is then sum over all such first order variational terms

$$H_{\text{str}} = \sum_{j,k} [\nabla V(R_{jk})]_0 \cdot \hat{\varepsilon} \cdot \mathbf{X}_k \equiv - \sum_j \sum_{\alpha} \hat{\Delta}_j^{\alpha} \hat{\varepsilon}^{\alpha}, \quad (4)$$

where we have introduced  $\hat{\Delta}_j = \mathbf{x}_j \mathbf{\Xi}_j$ , a dyadic whose components have different group symmetries denoted by  $\alpha$ , while  $\mathbf{\Xi}_j = \sum_k [\frac{1}{R_{jk}} \frac{\partial V_{jk}}{\partial R_{jk}}]_0 \mathbf{X}_k$  is the deformation potential. Here, we have assumed that the radial component of the gradient is the dominant one and neglected an irrelevant constant term. The former is a valid assumption as the total Coulomb attraction of the ions is more or less a central force [50–52].

The electronic configuration of this defect are given in Table I. Given the orbital symmetries of these states and the following table of symmetry for strain components the group theory can predict that the only non-zero irreducible representations of the  $\hat{\Delta}$  when sandwiched be-

tween two single-electron orbitals are:

$$C_{2v} : \begin{array}{c|ccc} \hat{\Delta}^{A_1} & a_1 & b_2 & b'_2 \\ \hline a_1 & \times & 0 & 0 \\ b_2 & 0 & \times & \times \\ b'_2 & 0 & \times & \times \end{array} \quad \hat{\Delta}^{B_2} : \begin{array}{c|ccc} & a_1 & b_2 & b'_2 \\ \hline a_1 & 0 & \times & \times \\ b_2 & \times & 0 & 0 \\ b'_2 & \times & 0 & 0 \end{array}, \quad C_{1h} : \begin{array}{c|ccc} \hat{\Delta}^{A'} & a_1 & b_2 & b'_2 \\ \hline a_1 & \times & \times & \times \\ b_2 & \times & \times & \times \\ b'_2 & \times & \times & \times \end{array}.$$

The effect of strain on multi-electron states is a non-equal shift in their energy levels imposed by the axial components of the strain as well as inducing an interaction between the states via the axial and non-axial strain components. The amount of shift only depends on the electronic states and its relations for the ground and excited states are  $\delta_0$ ,  $\delta_1$ , and  $\delta_2$ , respectively. The strain prompted inter-state interactions are much smaller than the energy difference between the levels, hence one neglects them in an adiabatic manner. The explicit form of the energy shifts are

$$\begin{aligned} \delta_0 &= \hat{\varepsilon}^{A'} [2\langle a_1 | \hat{\Delta}^{A'} | a_1 \rangle + \langle b_2 | \hat{\Delta}^{A'} | b_2 \rangle], \\ \delta_1 &= \hat{\varepsilon}^{A_1} [2\langle b_2 | \hat{\Delta}^{A_1} | b_2 \rangle + \langle a_1 | \hat{\Delta}^{A_1} | a_1 \rangle], \\ \delta_2 &= \hat{\varepsilon}^{A'} [2\langle a_1 | \hat{\Delta}^{A'} | a_1 \rangle + \langle b'_2 | \hat{\Delta}^{A'} | b'_2 \rangle]. \end{aligned}$$

In the main text we have adopted the approximation that  $\hat{\varepsilon}^{A'} \langle \cdot | \hat{\Delta}^{A'} | \cdot \rangle \approx \hat{\varepsilon}^{A_1} \langle \cdot | \hat{\Delta}^{A_1} | \cdot \rangle$  which is reasonable owing to the fact that  $C_{1h}$  is a subgroup of  $C_{2v}$  and that the molecular orbitals retain their form.

## B. Details on DFT calculations

The calculations are performed based on the density functional theory (DFT) implemented in Vienna ab initio simulation package (VASP). [53, 54] Projector augmented wave (PAW) is used to separate the valence electrons from the core part. The energy cutoff for the expansion of plane-wave basis set was set to 450 eV which is enough to provide accurate result. The screened hybrid density functional of Heyd, Scuseria, and Ernzerhof (HSE) [55] is used to calculate to band gap and defect levels. Within this approach, the short-range exchange potential is described by mixing with part of nonlocal Hartree-Fock exchange and this also provides reasonable geometry optimization of dynamic Jahn-Teller system. The HSE hybrid functional with mixing parameter of 0.32 closely reproduces the experimental band gap at 5.9 eV. To apply the strain along the parallel and perpendicular directions to the  $C_2$  axis, a  $9 \times 5\sqrt{3}$  supercell is constructed through changing the basis to the orthorhombic structure. The perfect supercell contains 160 atoms which is sufficient to avoid the defect-defect interaction, and the single  $\Gamma$ -point scheme is converged for the k-point sampling for the Brillouin zone. The coordinates of atoms are allowed to relax until the force is less than 0.01 eV/Å. The excited state was calculated within  $\Delta$ SCF method [56] that we previously applied to point defects in  $h$ -BN too [27].

## AUTHOR CONTRIBUTION

SL carried out the DFT calculations under the supervision of JPC, AH, and AG. MA developed the group theory analysis with MBP. PU and GT developed and applied the electron-phonon coupling theory on the defect under the supervision of AG. All authors contributed to the discussion and writing the manuscript. AG conceived and led the entire scientific project.

## COMPETING INTERESTS

The authors declare that there are no competing interests.

## DATA AVAILABILITY

The data that support the findings of this study are available from the corresponding author upon reasonable

request.

## ACKNOWLEDGMENTS

AG acknowledges the Hungarian NKFIH grant No. KKP129866 of the National Excellence Program of Quantum-coherent materials project, the National Quantum Technology Program (Grant No. 2017-1.2.1-NKP-2017-00001), and the EU H2020 Quantum Technology Flagship project ASTERIQS (Grant No. 820394). MBP acknowledges support from the ERC Synergy grant BioQ (Grant No. 319130), the EU H2020 Quantum Technology Flagship project ASTERIQS (Grant No. 820394), the EU H2020 Project Hyperdiamond (Grant No. 667192) and the BMBF via NanoSpin and DiaPol. MA acknowledges support by INSF (Grant No. 98005028).

- 
- [1] A. Srivastava, M. Sidler, A. V. Allain, D. S. Lembke, A. Kis, and A. Imamoglu, *Nat. Nanotechnol.* **10**, 491 (2015).
  - [2] C. Chakraborty, L. Kinnischtzke, K. M. Goodfellow, R. Beams, and A. N. Vamivakas, *Nat. Nanotechnol.* **10**, 507 (2015).
  - [3] C. Palacios-Berraquero, M. Barbone, D. M. Kara, X. Chen, I. Goykhman, D. Yoon, A. K. Ott, J. Beitzner, K. Watanabe, T. Taniguchi, A. C. Ferrari, and M. Atatüre, *Nat. Commun.* **7**, 12978 (2016).
  - [4] F. Xia, H. Wang, D. Xiao, M. Dubey, and A. Ramasubramaniam, *Nat. Photon.* **8**, 899 (2014).
  - [5] G. Clark, J. R. Schaibley, J. Ross, T. Taniguchi, K. Watanabe, J. R. Hendrickson, S. Mou, W. Yao, and X. Xu, *Nano Lett.* **16**, 3944 (2016).
  - [6] R.-J. Shiue, D. K. Efetov, G. Grosso, C. Peng, K. C. Fong, and D. Englund, *Nanophotonics* **6**, 1329 (2017).
  - [7] S. Lee, J.-S. Yeo, Y. Ji, C. Cho, D.-Y. Kim, S.-I. Na, B. H. Lee, and T. Lee, *Nanotechnology* **23**, 344013 (2012).
  - [8] A. Abderrahmane, P. J. Ko, T. V. Thu, S. Ishizawa, T. Takamura, and A. Sandhu, *Nanotechnology* **25**, 365202 (2014).
  - [9] X. Li, J. Yin, J. Zhou, and W. Guo, *Nanotechnology* **25**, 105701 (2014).
  - [10] T. T. Tran, K. Bray, M. J. Ford, M. Toth, and I. Aharonovich, *Nat. Nanotechnol.* **11**, 37 (2016).
  - [11] M. Abdi, M.-J. Hwang, M. Aghtar, and M. B. Plenio, *Phys. Rev. Lett.* **119**, 233602 (2017).
  - [12] I. Aharonovich, D. Englund, and M. Toth, *Nat. Photon.* **10**, 631 (2016).
  - [13] D. Golberg, Y. Bando, Y. Huang, T. Terao, M. Mitome, C. Tang, and C. Zhi, *ACS Nano* **4**, 2979 (2010).
  - [14] T. T. Tran, C. Elbadawi, D. Totonjian, C. J. Lobo, G. Grosso, H. Moon, D. R. Englund, M. J. Ford, I. Aharonovich, and M. Toth, *ACS Nano* **10**, 7331 (2016).
  - [15] T. T. Tran, C. Zachreson, A. M. Berhane, K. Bray, R. G. Sandstrom, L. H. Li, T. Taniguchi, K. Watanabe, I. Aharonovich, and M. Toth, *Phys. Rev. Applied* **5**, 034005 (2016).
  - [16] N. R. Jungwirth, B. Calderon, Y. Ji, M. G. Spencer, M. E. Flatté, and G. D. Fuchs, *Nano Lett.* **16**, 6052 (2016).
  - [17] L. J. Martinez, T. Pelini, V. Waselowski, J. R. Maze, B. Gil, G. Cassaboies, and V. Jacques, *Phys. Rev. B* **94**, 121405(R) (2016).
  - [18] A. W. Schell, T. T. Tran, H. Takashima, S. Takeuchi, and I. Aharonovich, *ACS Photonics* **4**, 761 (2017).
  - [19] Z. Shotan, H. Jayakumar, C. R. Consideine, M. Mackoitt, H. Fedde, J. Wrachtrup, A. Alkauskas, M. W. Doherty, V. M. Menon, and C. A. Meriles, *ACS Photonics* **3**, 2490 (2016).
  - [20] N. R. Jungwirth and G. D. Fuchs, *Physical Review Letters* **119**, 057401 (2017).
  - [21] X. Li, G. D. Shepard, A. Cupo, N. Camporeale, K. Shayan, Y. Luo, V. Meunier, and S. Strauf, *ACS Nano* **11**, 6652 (2017).
  - [22] A. L. Exarhos, D. A. Hopper, R. R. Grote, A. Alkauskas, and L. C. Bassett, *ACS Nano* **11**, 3328 (2017).
  - [23] L. Museum, E. Feldbach, and A. Kanaev, *Phys. Rev. B* **78**, 155204 (2008).
  - [24] R. Bourrellier, S. Meuret, A. Tararan, O. Stephan, M. Kociak, L. H. G. Tizei, and A. Zobelli, *Nano Lett.* **16**, 4317 (2016).
  - [25] T. Q. P. Vuong, G. Cassaboies, P. Valvin, A. Ouerghi, Y. Chassagneux, C. Voisin, and B. Gil, *Phys. Rev. Lett.* **117**, 097402 (2016).
  - [26] S. A. Tawfik, S. Ali, M. Fronzi, M. Kianinia, T. T. Tran, C. Stampfl, I. Aharonovich, M. Toth, and M. J. Ford, *Nanoscale* **9**, 13575 (2017).
  - [27] M. Abdi, J.-P. Chou, A. Gali, and M. B. Plenio, *ACS Photonics* **5**, 1967 (2018).

- [28] L. Weston, D. Wickramaratne, M. Mackoite, A. Alkauskas, and C. G. Van de Walle, *Phys. Rev. B* **97**, 214104 (2018).
- [29] M. E. Turiansky, A. Alkauskas, L. C. Bassett, and C. G. Van de Walle, *Phys. Rev. Lett.* **123**, 127401 (2019).
- [30] M. Mackoite-Sinkevicius, M. Maciaszek, C. G. Van de Walle, and A. Alkauskas, *Appl. Phys. Lett.* **115**, 212101 (2019).
- [31] N. Chejanovsky, M. Rezai, F. Paolucci, Y. Kim, T. Rendler, W. Rouabeh, F. F. de Oliveira, P. Herlinger, A. Denisenko, S. Yang, I. Gerhardt, A. Finkler, J. H. Smet, and J. Wrachtrup, *Nano Lett.* **16**, 7037 (2016).
- [32] J. Ziegler, R. Klaiss, A. Blaikie, D. Miller, V. R. Horowitz, and B. J. Aleman, *Nano Lett.* **19**, 2121 (2019).
- [33] J. R. Toledo, D. B. de Jesus, M. Kianinia, A. S. Leal, C. Fantini, L. A. Cury, G. A. M. Safar, I. Aharonovich, and K. Krambrock, *Phys. Rev. B* **98**, 155203 (2018).
- [34] A. L. Exarhos, D. A. Hopper, R. N. Patel, M. W. Doherty, and L. C. Bassett, *Nat. Commun.* **10**, 222 (2019).
- [35] N. Chejanovsky, A. Mukherjee, Y. Kim, A. A. Denisenko, A. Finkler, T. Taniguchi, K. Watanabe, D. B. R. Dasari, J. H. Smet, and J. J. Wrachtrup, *arXiv:1906.05903*.
- [36] A. Gottscholl, M. Kianinia, V. Soltamov, C. Bradac, C. Kasper, K. Krambrock, A. Sperlich, M. Toth, I. Aharonovich, and V. Dyakonov, (2019), *arXiv:1906.03777 [physics.optics]*.
- [37] M. E. Turiansky, A. Alkauskas, L. C. Bassett, and C. G. Van de Walle, *Phys. Rev. Lett.* **123**, 127401 (2019).
- [38] A. Bommer and C. Becher, *Nanophotonics* **8**, 2041 (2019).
- [39] F. Hayee, L. Yu, J. L. Zhang, C. J. Ciccarino, M. Nguyen, A. F. Marshall, I. Aharonovich, J. Vučković, P. Narang, T. F. Heinz, and J. A. Dionne, (2019), *arXiv:1901.05952 [cond-mat.mtrl-sci]*.
- [40] G. Grosso, H. Moon, B. Lienhard, S. Ali, D. K. Efetov, M. M. Furchi, P. Jarillo-Herrero, M. J. Ford, I. Aharonovich, and D. Englund, *Nat. Commun.* **8**, 705 (2017).
- [41] M. Abdi and M. B. Plenio, *Phys. Rev. A* **98**, 040303(R) (2018).
- [42] M. Abdi and M. B. Plenio, *Phys. Rev. Lett.* **122**, 023602 (2019).
- [43] A. Sajid, J. R. Reimers, and M. J. Ford, *Phys. Rev. B* **97**, 064101 (2018).
- [44] F. Wu, T. J. Smart, J. Xu, and Y. Ping, *Phys. Rev. B* **100**, 081407 (2019).
- [45] J. R. Reimers, A. Sajid, R. Kobayashi, and M. J. Ford, *J. Chem. Theory Comput.* **14**, 1602 (2018).
- [46] G. Noh, D. Choi, J.-H. Kim, D.-G. Im, Y.-H. Kim, H. Seo, and J. Lee, *Nano Lett.* **18**, 4710 (2018).
- [47] I. Bersuker, *The Jahn-Teller Effect* (Cambridge University Press, 2006).
- [48] G. m. H. Thiering and A. Gali, *Phys. Rev. B* **96**, 081115 (2017).
- [49] V. Ivády, G. Barcza, G. Thiering, S. Li, H. Hamdi, O. Legeza, J.-P. Chou, and A. Gali, *arXiv:1910.07767 [cond-mat]* (2019).
- [50] L. Boldrin, F. Scarpa, R. Chowdhury, and S. Adhikari, *Nanotechnology* **22**, 505702 (2011).
- [51] Q. Peng, W. Ji, and S. De, *Comput. Mater. Sci.* **56**, 11 (2012).
- [52] S. K. Singh, M. Neek-Amal, S. Costamagna, and F. M. Peeters, *Phys. Rev. B* **87**, 184106 (2013).
- [53] G. Kresse and J. Furthmüller, *Phys. Rev. B* **54**, 11169 (1996).
- [54] G. Kresse and J. Furthmüller, *Comput. Mater. Sci.* **16**, 15 (1996).
- [55] J. Heyd, G. E. Scuseria, and M. Ernzerhof, *J. Chem. Phys.* **118**, 8207 (2003).
- [56] A. Gali, E. Janzén, P. Deák, G. Kresse, and E. Kaxiras, *Phys. Rev. Lett.* **103**, 186404 (2009).